

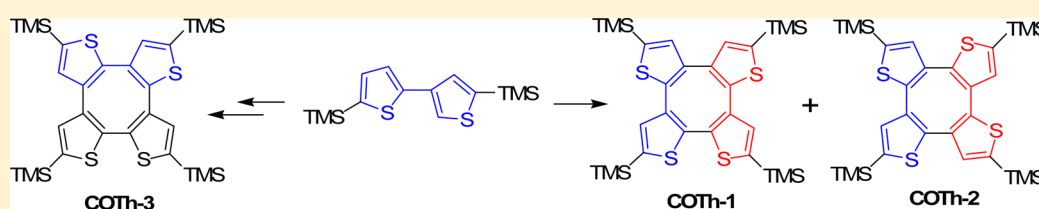
Synthesis and Characterization of Cyclooctatetrathiophenes with Different Connection Sequences

Yong Wang,^{†,‡,||} Jinsheng Song,^{*,†,||} Li Xu,[‡] Yuhe Kan,^{§,*} Jianwu Shi,[†] and Hua Wang^{*,†}

[†]Key Lab for Special Functional Materials of Ministry of Education and [‡]College of Chemistry and Chemical Engineering, Henan University, Kaifeng 475004, China

[§]Jiangsu Province Key Laboratory for Chemistry of Low Dimensional Materials, School of Chemistry and Chemical Engineering, Huaiyin Normal University, Huaian 223300, China

S Supporting Information



ABSTRACT: Based on the selectivity of deprotonation of 5,5'-bistrimethylsilyl-2,3'-bithiophene (**4**) in the presence of *n*-BuLi, three new cyclooctatetrathiophenes (COThs), COTh-1, COTh-2, and COTh-3 have been efficiently developed via intermolecular or intramolecular cyclizations. Their crystal structures clearly show that the different connectivity sequence of the thiophene rings in the molecules. The CV data and UV–vis absorbance spectra of COThs are also described. In addition, the time-dependent density functional theory (TDDFT) calculations accurately reproduce experimental observations and afford band assignment.

INTRODUCTION

In recent years, unusual topologies of polycyclic hydrocarbons have been the subject of considerable attention.^{1–3} Cyclooctatetraene (COT) is one of the classical flexible π -conjugated skeletons, which has an 8π annulene possessing an inherently nonplanar saddle-shaped geometry with D_{2d} symmetry. The planar structures can be obtained according to Hückel's rule via oxidation and/or reduction reactions. Because of the angle strain and antiaromaticity, the planar conformation of COT structure is unstable and prefers to keep the skeleton in the nonplanar conformations through the tub-to-tub inversion. Based on this interesting behavior, many COT-based materials have been designed and synthesized as cavity-size-controlled cage molecules,⁴ electromechanical actuators,⁵ buckycatchers,⁶ and molecular tweezers.⁷ After phenyl-fused COT was reported by Rapson in 1943,⁸ various sophisticated COT structures have been designed and synthesized, such as the thiophene-, furan-, pyrimidine-, and benzothiophene-fused COTs.⁹ Recently, Yamaguchi reported the synthesis and characterization of thiazole-fused COT,¹⁰ whose configuration can be changed from the tub-shaped skeleton to a planar form via reduction or oxidation according to the Hückel's rule.

Among the COT family, an interesting member, thiophene-fused COT, namely cyclooctatetrathiophene, was first reported by Kauffmann in 1978.^{9a} In our previous work,^{9b} we reported the structure of COTh-4 as shown in Figure 1, which is composed of four thienylene moieties and possesses the general COT characters. It has been considered as one of the classical flexible π -conjugated skeletons based on their interesting

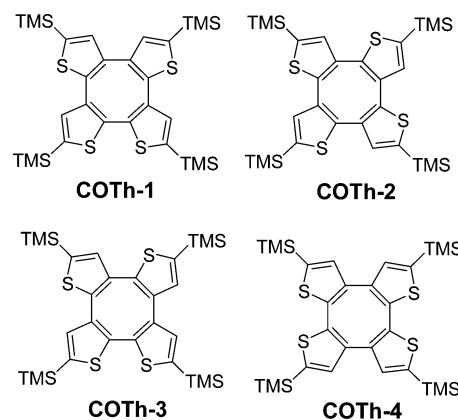


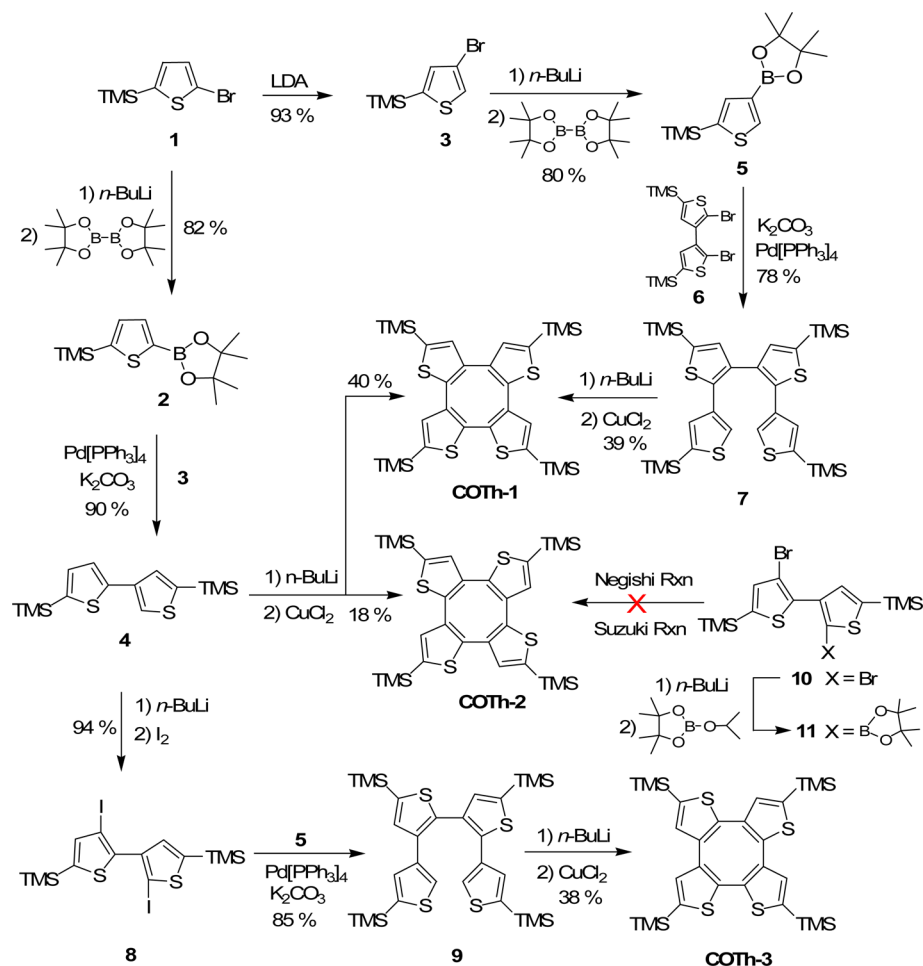
Figure 1. Molecular structures of COTh-1 to COTh-4.

dynamic molecular motions.^{5–7} With four peripheral α -positions available on the parent COTh-4, a variety of derivatives with different functional groups can be synthesized, which could be used as a new class of organic electronic materials in single-molecular electromechanical actuators reported by Marsella.^{5,11} In 2009, our group reported dithieno[2,3-*b*:3',2'-*d*]thiophene-fused COT-forming double helix.¹² This sophisticated structure not only possesses the general COT character but also shows a double-helical

Received: February 5, 2014

Published: February 13, 2014

Scheme 1. Synthetic Route to COTh-1, COTh-2, and COTh-3



configuration, which might be used as a chiral catalyst for organic synthesis and an organic semiconductor.

Although many interesting works based on COTh-4 have been reported, it is rare to see a report of the isomers of COTh with a different connection manner of the four thiophene moieties according to our knowledge. These isomers may enrich the members of the COT family and expand the abundant study in both organic synthesis and organic electronics. Herein, we describe the efficient synthesis of three new isomers, COTh-1, COTh-2, and COTh-3 (Figure 1) via intermolecular or intramolecular cyclizations based on the selectivity of deprotonation of 4 in the presence of *n*-BuLi. Their molecular structures have been confirmed by single-crystal analyses, and the different connectivity sequences of the thiophene rings in these molecules are clearly shown. In addition, the UV-vis absorbance spectra, CV data, and TDDFT quantum calculations of the title compounds have been described.

RESULTS AND DISCUSSION

Syntheses of COThs. The syntheses of COTh-1, COTh-2, and COTh-3 are shown in Scheme 1. Two main routes were utilized. Starting from 2-bromo-5-trimethylsilylthiophene (**1**),¹³ *n*-BuLi was used with **1** for Br/Li exchange at $-78\text{ }^{\circ}\text{C}$, and subsequent addition of bis(pinacolato)diboron, 2-(4,4,5,5-tetramethyl-1,3,2-dioxaborolan-2-yl)-5-trimethylsilylthiophene (**2**), was obtained in a yield of 82%. 3-Bromo-5-trimethylsilyl-

thiophene (**3**) was prepared from **1** by a bromine dance (BD) reaction¹⁴ in a high yield of 93%. Compound **4** is a crucial building block in the synthesis of COThs (Scheme 1), and it was prepared by palladium-catalyzed Suzuki–Miyaura cross-coupling of **2** with **3** in 90% yield. During this synthetic process, the experimental results revealed that the deprotonation of **4** with *n*-BuLi (2 equiv) showed high selectivity. Only the protons on the α -position (C2) of the right thiophene ring and the β -position (C3) of the left thiophene ring can be removed to form intermediate 4-Li₂. After CuCl₂ oxidation, two isomers, COTh-1 and COTh-2 can be obtained by intermolecular cyclizations in one pot with yields of 40% and 18%, respectively. Although their molecular polarities are very similar, COTh-1 and COTh-2 still can be separated by column chromatography on silica gel with petroleum ether (60–90 °C) as eluent.

In order to avoid the tough separation of the isomers, the precursors (**7** and **9**) bearing two thiophene moieties linking to bithiophenes are designed as shown in Scheme 1. COTh-1 and COTh-3 can be obtained by intramolecular cyclizations of **7** and **9**, respectively. As for making COTh-1, starting from **3**, its reaction with *n*-BuLi at $-78\text{ }^{\circ}\text{C}$ and subsequent addition of bis(pinacolato)diboron afforded 3-(4,4,5,5-tetramethyl-1,3,2-dioxaborolan-2-yl)-5-trimethylsilylthiophene (**5**) in a yield of 80%. Then the Suzuki–Miyaura cross-coupling of **5** and 2,2'-dibromo-5,5'-bis(trimethylsilyl)-3,3'-bithiophene (**6**)^{9b} took place to afford **7** in a yield of 78%. After deprotonation of **7**

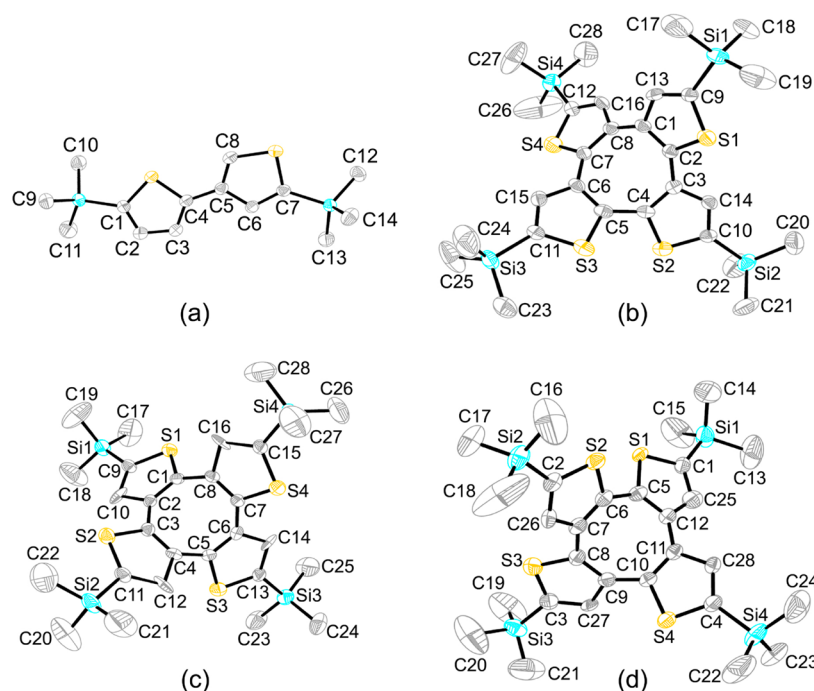


Figure 2. Crystal structures for 4 (a), COTh-1 (b), COTh-2 (c), and COTh-3 (d). Carbon and sulfur atoms are depicted with thermal ellipsoids set at the 30% probability level, and all hydrogen atoms are omitted for clarity.

with *n*-BuLi and subsequent CuCl₂ oxidation reaction, COTh-1 was obtained in a yield of 39%. The similar synthetic route was employed for making COTh-3. With 4 as the raw material, 3,2'-diiodo-5,5'-bis(trimethylsilyl)-2,3'-bithiophene (8) was obtained in a yield of 94% by quenching intermediate 4-Li₂ with iodine. Compound 9 was obtained in a yield of 85% via Suzuki–Miyaura cross-coupling between 8 and 5. COTh-3 was obtained in 38% yield via the deprotonation of 9 with *n*-BuLi and subsequent intramolecular CuCl₂ oxidation reaction. In order to increase the synthetic yield of COTh-2, both Negishi and Suzuki cross couplings were attempted on the basis of the corresponding precursors of 10¹⁵ and 11 (Scheme 1), respectively. However, the crude products were very complicated with main content of polymerization, and trace title product was observed.

Crystal Structures of COThs. The molecular structures of COTh-1, COTh-2, COTh-3, and 4 are confirmed by single-crystal X-ray analyses (Figure 2). They belong to monoclinic space group *P*2(1)/*n*, orthorhombic space group *Pna*2(1), triclinic space group *P*-1, and orthorhombic space group *P*2(1)2(1)2(1), respectively. In 4, the two thiophenes are slightly distorted from a coplanar arrangement. The dihedral angle between the two thiophene moieties is 6.4°, and the torsion angle is 6.2° (C3–C4–C5–C6). COTh-1, COTh-2, and COTh-3 reveal their saddle-shaped structures wherein the central COT moieties are in the tub conformations.

In the crystal packing structures of COTh-1 and COTh-3, the disorders with the approximate occupancy ratios of 65:35 and 57:43 are found, respectively, while X-ray crystallographic data for a single crystal of COTh-2 show unequivocal evidence of solvent inclusion via interaction between the molecule of solvent (CHCl₃) and substrate with a ratio of 1:1. For the inner angles (α) of the central eight-membered ring, the average values in the X-ray structures of COTh-1, COTh-2, and COTh-3 are 129.0°, 127.5°, and 128.2°, respectively, which are close to the inner angle of COTh-4 (128.4°).^{9b}

For clarity, certain parameters are defined (Figure 3). The average bent angle and dihedral angle between the two moieties

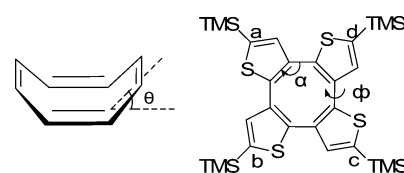


Figure 3. Notations used to describe the parent COTh-2 scaffold.

of adjacent thiophene are denoted as θ and Φ ,⁵ respectively. In addition, the distance between carbons Ca...Cc or Cb...Cd is denoted as *D*.^{5b} Here, a, b, c, and d are denoted as the four α -carbons of the four thiophene rings (see Figure 3). The structural data from X-ray analysis are summarized in Table 1.

Table 1. Structural Data from X-ray Analysis for COThs


compd	α (deg)		θ (deg)		Φ (deg)	<i>D</i> (Å)	HOMO–LUMO gap (eV)
	crystal	theory	crystal	theory			
COTh-1	129.0	128.0	36.1	40.0	41.5	7.19	2.92
COTh-2	127.5	127.4	39.9	40.1	50.5	6.84	3.07
COTh-3	128.2	128.0	38.1	40.4	43.9	7.04	2.97
COTh-4	128.4	127.4	37.7	40.5	43.5	7.10	2.98

The tub structure of the COT moiety in COTh-1 is shallowest in these COThs. The average bent angles θ (as listed in Table 1) of the COT skeleton in COTh-1, COTh-2, and COTh-3 are 36.1°, 39.9°, and 38.1°, respectively. The dihedral angle (Φ) in the structure of COTh-1 is 41.5°, which is smaller than that of the other two COThs, while for the distance (*D*) in the structure of COTh-1 it is the largest (7.19 Å) among the COThs. There is a direct relationship between Φ and *D*, such

that a decrease in Φ mandates an increase in D and vice versa.^{5b} In their crystal forms, **COTh-1**, **COTh-2**, and **COTh-3** do not stack in columnar forms¹⁰ (see Figure S31, Supporting Information). The intermolecular parallel thiophene ring distances of **COTh-1**, **COTh-2**, and **COTh-3** are 10.31, 12.88, and 12.83 Å, respectively, while the distance of 13.31 Å is observed for **COTh-4**. π -Stacking is absent within the crystal packing of the four isomers. The weak packing disfavors crystallization and gives rise to good solubility. These results indicated that the different connection manner of the four thienylene moieties can slightly influence the packing style of these saddle-shaped molecules. The molecular symmetry in solution on the NMR timescale corresponds to the approximate molecular symmetry determined by crystallography.

Quantum Chemistry Calculation and Absorbance Spectra of COThs. The inversion barriers of **COTh-1**, **COTh-2**, **COTh-3**, and **COTh-4** are 28.6, 27.0, 28.6, and 30.5 kcal/mol, respectively, based on the quantum chemical calculations at B3LYP/6-31G* level (see Table 2). Their slight

Table 2. Energetic, Structural, and Magnetic Characteristics of COT and COTh 1–4 Model Compounds Calculated by the B3LYP/6-31G* Level of theory

Compounds	Inversion barrier (kcal/mol)	 bent angle (°)	NICS(0) ^a (ppm)	NICS(0) ^b (ppm)	Dipole moment (Debye)
COTh-1	28.6	40.0	4.0	15.0	1.31
COTh-2	27.0	40.1	4.7	15.3	0.00
COTh-3	28.6	40.4	3.9	15.3	0.86
COTh-4	30.5	40.5	3.6	14.7	0.11
COT	10.9	39.4	5.0	41.5(+42.1) ^c	0.05

^aThe NICS values at the center of the 8-membered ring in the ground state were calculated at the B3LYP/6-311+G(d,p) level of theory based on the B3LYP/6-31G(d) optimized structures. ^bThe NICS values at the center of the 8-membered ring in the transition state (TS) were calculated at the B3LYP/6-311+G(d,p) level of theory based on the B3LYP/6-31G(d) optimized structures. ^cData in parentheses from ref 10.

differences could be attributed to the different connectivity sequence of the thiophene rings. However, these values are larger than those of thiazole-fused **COT** derivatives (6.6–22.4 kcal/mol),¹⁰ which means these **COThs** possess high structural stability, and it is not easy to proceed to the structural inversion. The calculated dipole moments for **COThs** are in line with expectations (Table 2), in which the dipole moment for **COTh-1** (1.31 D) is higher than those for other isomers and **COT** (0.05 D). The nucleus-independent chemical shift (NICS) calculation was also performed on these molecules, and all **COT** rings in these molecules at ground states (GS) exhibit the antiaromatic paratropicity with the NICS (0) value from 3.6 to 4.7. The NICS values are almost identical to that of parent **COT**, suggesting that sulfur atoms of thiophenes do not substantially affect the NICS values of the central ring. In the case of the transition state (TS), there was an enhancement of the antiaromatic paratropicity of the **COT** rings in the

molecules with the NICS (0) value around 15.0 for all of the **COThs**, which are less than that of parent planar **COT** (41.5).

According to the literature,¹⁶ a narrowing of the HOMO–LUMO gap could be found with decreasing bent angle of the **COT** rings. Similar results are also discovered in our molecules, with the bent angle increasing in the order $\theta_{\text{COTh-1}} < \theta_{\text{COTh-4}} \approx \theta_{\text{COTh-3}} < \theta_{\text{COTh-2}}$, and the HOMO–LUMO gaps are derived from the band edge absorption decreased in the order **COTh-2** > **COTh-3** \approx **COTh-4** > **COTh-1**. From the notation structure, it is easy to understand that the structure with smaller θ and Φ angles should have better conjugation in the molecule, generate a lower HOMO–LUMO gap, and cause the absorption curve red-shift, finally. From the discussion above, we can conclude that the character of the saddle shape for the **COTh** molecules can be fine-tuned by the structure design of the sulfur position in the molecules.

COThs possess homologous cross-conjugated π -systems in which adjacent thiophene rings are alternatively connected, analogously to the linkages in tetraphenylenes.¹⁷ The out-of-plane twisting between the adjacent thiophene rings and the possible cross-conjugation may affect the delocalization in macrocyclic oligothiophenes.^{9b,18} From the absorbance spectra of **COThs** (Figure 4), we can see that all the four **COThs**

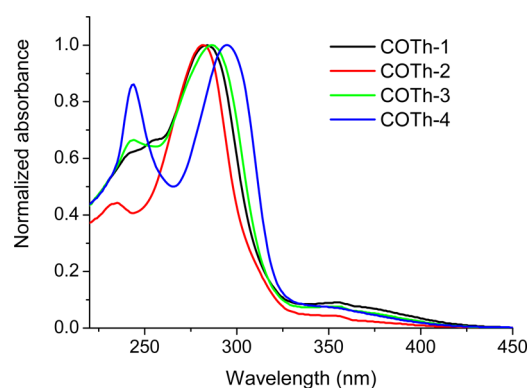


Figure 4. Normalized absorbance spectra of **COThs** in chloroform.

showed similar absorbance curves, and there were three absorption bands (bands I–III), which were located in the regions of 220–260, 260–320, and 330–400 nm, respectively. Similar maximum absorbance peaks (λ_{max}) are definitely observed as 284, 282, 287, and 295 nm for **COTh-1**, **COTh-2**, **COTh-3**, and **COTh-4**, respectively. Such absorbance behaviors imply that the connectivity sequence of the thiophene rings in the **COTh** molecules can only slightly change the conjugations of **COThs**.

To obtain further insight into the effect of molecular structure and electron distribution on the spectroscopic properties of the **COThs**, their electronic structure and excited-state calculations were performed by the TD-DFT/PCM approach at the 6-31+G(d,p) level. As shown in Figure S40 (Supporting Information), it can be seen that TD-B3LYP/PCM results accurately reproduce the peak position and relative intensity of the measured whole absorption bands. The vertical excitation energies, oscillator strengths, and transition contributions of the most important states are presented in Table 3.

The lower intensity absorption band I located at 230 nm is associated with the mixed transitions from the higher energy excitation (see Tables S1–S4, Supporting Information). The

Table 3. Selected Computational Absorption Energies (nm, eV in parentheses), Oscillator Strength (f), and Transition Nature in Chloroform Solvent at the TD-B3LYP/6-31+G(d,p) Level of theory

	state	λ	f	transition contributions	μ_{eg}^2
COTh-1	$S_0 \rightarrow S_1$	384.7 (3.22)	0.0338	HOMO→LUMO (99%)	0.43
	$S_0 \rightarrow S_4$	287.5 (4.31)	0.2318	HOMO→L+1 (70%)	2.19
	$S_0 \rightarrow S_5$	281.7 (4.40)	0.2194	HOMO→L+2 (55%)	2.03
COTh-2	$S_0 \rightarrow S_1$	382.2 (3.24)	0.0000	HOMO→LUMO (99%)	0.00
	$S_0 \rightarrow S_5$	274.7 (4.51)	0.3692	HOMO→L+1 (82%)	3.34
	$S_0 \rightarrow S_6$	274.5 (4.52)	0.3667	HOMO→L+2 (82%)	3.31
COTh-3	$S_0 \rightarrow S_1$	382.9 (2.64)	0.0206	HOMO→LUMO (99%)	0.26
	$S_0 \rightarrow S_4$	287.3 (4.32)	0.3474	HOMO→L+1 (70%)	3.28
COTh-4	$S_0 \rightarrow S_1$	380.1 (3.26)	0.0133	HOMO→LUMO (99%)	0.17
	$S_0 \rightarrow S_3$	292.6 (4.24)	0.4401	HOMO→L+1 (74%)	4.24

corresponding calculations for band II give rise to broadly strong peaks in a range of 260–320 nm, which are in agreement with the experimental results. The largest contributions in this very intense absorption are attributed to the $S_0 \rightarrow S_3$, S_4 , or S_5 transition, which is dominated by a HOMO to LUMO+1 component (in Table 3). It is noteworthy that there is a slight bathochromic shift (~ 10 nm) observed for the λ_{max} value of COTh-4 compared to other COThs, and this can be ascribed to the alignment of the LUMO+1 energy (Figure S41, Supporting Information). For all COThs, the observed lowest energy absorption bands (band III) are associated to the predicted $S_0 \rightarrow S_1$ transitions, and the extremely weak absorption can be assigned as a “forbidden” HOMO–LUMO transition

due to small transition dipole moments, especially in COTh-2 (Table 3). The transition orbitals contributing to these bands were determined using natural transition orbital and charge difference density analysis. Taking COTh-1, for example, Figure 5 demonstrates the assignment of the most important transitions corresponding to the three absorption bands (for other COThs, see Figures S42–S45 in the Supporting Information).

Cyclic Voltammetry Data of COThs. The cyclic voltammetry (CV) were utilized to determine the electrochemical properties of the COThs in CH_2Cl_2 with Ag/AgCl electrode as the reference electrode. All four isomers showed one similar oxidation peak, which was proved to be a quasi-reversible oxidation process (Figure S32, Supporting Information). The oxidation peaks were located in the regions of 0.74–0.78 V (vs Fc/Fc⁺), and no redox process occurred at negative potential within the scanning window of 0 to –2.0 V (vs Ag/AgCl). These values were similar, which revealed that the connectivity sequences of the thiophene moieties have little influence on the redox properties and the central COT moiety endows these skeletons with high redox stability.^{10,19}

Meanwhile, from the cyclic voltammograms results at different scan speeds (from 25 to 175 mV/s), it is easy to determine that peak current increased linearly with the scan rate, which indicated that the electrode process was controlled by adsorption.^{20–22} With the Laviron method,²⁰ the number of electrons (n) occurred in the oxidation process of each COTh was calculated to be 2 (Figures S33–35, Supporting Information).

CONCLUSION

In summary, three new COThs with different connectivity sequences of the thiophene rings have been efficiently synthesized via intermolecular and intramolecular cyclizations based on the high deprotonation selectivity of **4** in the presence of *n*-BuLi. It is interesting to mention that COTh-1 and COTh-2 can be made in one pot with good yields. The molecular structures of these COThs were confirmed by single-

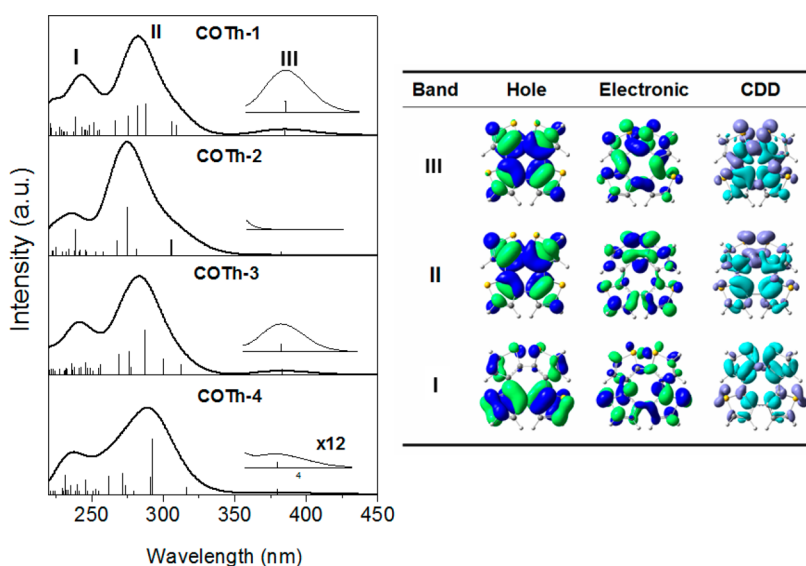


Figure 5. Calculated optical absorption spectra of model compounds COTh-1 to COTh-4 in chloroform solution within TD-DFT/PCM approaches based on B3LYP/6-31+G(d,p) level of theory (left). Natural transition orbitals (NTOs) and charge difference densities (CDDs) for assigning the transitions corresponding to the main absorption band of COTh-1 (right). Cyan and violet colors represent the decrease and increase of electron in CDD map, respectively.

crystal structures and based on which quantum calculations were also set up. By virtue of the structural differences, the absorbance spectra, the CV data, and the crystal structural data of COThs exhibited slight differences. These new structures of COThs offer more chances to adjust the novel saddle-shaped COT molecules, such as novel oligomers based on the four peripheral α -positions available on the parent COThs.²³ Besides the high interest in organic synthesis, these new COThs might provide more and novel opportunities devoted to a wide field such as supramolecular chemistry and organic electronics.

EXPERIMENTAL SECTION

Synthesis of 2-(4,4,5,5-Tetramethyl-1,3,2-dioxaborolan-2-yl)-5-trimethylsilylthiophene (2). *n*-BuLi (2.34 M in hexane, 1.65 mL, 3.86 mmol, 1.0 equiv) was added to 2-bromo-5-trimethylsilylthiophene (1) (0.8660 g, 3.68 mmol, 1.0 equiv) in THF (30 mL) at -78°C . After 2 h at -78°C , the reaction mixture was treated with bis(pinacolato)diboron (1.0280 g, 4.05 mmol, 1.1 equiv, dissolved in 15 mL of THF) and then warmed slowly to ambient temperature overnight. The reaction mixture was quenched with water, extracted with chloroform (3 \times 40 mL), and finally dried over anhydrous MgSO_4 . After the solvent was removed in vacuo, the residue was purified by column chromatography on silica gel via gradient elution using the solvent mixture (5:1 petroleum ether to chloroform) as eluent to yield 2 (0.8517 g, 82%) as a white solid. Mp: 89–90 $^\circ\text{C}$ (lit.²⁴ mp 61–62 $^\circ\text{C}$). ^1H NMR (CDCl_3 , 400 MHz): δ 7.69 (d, J = 3.2 Hz, 1H), 7.33 (d, J = 3.2 Hz, 1H), 1.34 (s, 12H), 0.32 (s, 9H). ^{13}C NMR (100 MHz, CDCl_3): δ 148.45, 137.86, 135.00, 84.02, 24.73, -0.11 . IR (KBr): 3054, 2982, 2958, 2897 (C–H) cm^{-1} . HRMS (EI^+): m/z calcd for $[\text{C}_{13}\text{H}_{23}\text{O}_2\text{Si}^{10}\text{B}]$ 281.1317, found 281.1314.

Synthesis of 5,5'-Bistrimethylsilyl-2,3'-bithiophene (4). Compound 2 (1.4842 g, 5.26 mmol 1.2 equiv), 3-bromo-5-trimethylsilylthiophene (3) (1.0312 g, 4.38 mmol 1.0 equiv), K_2CO_3 (1.5148 g, 10.96 mmol, 2.5 equiv), and $\text{Pd}(\text{PPh}_3)_4$ (0.1013 g, 87.66 μmol , 0.02 equiv) were added into THF (20 mL) and water (2 mL) under argon. The mixture was stirred for 15 h at 100 $^\circ\text{C}$. The reaction mixture was extracted with chloroform (3 \times 35 mL) and finally dried over anhydrous MgSO_4 . After the solvent was removed in vacuo, the residue was purified by column chromatography on silica gel with petroleum ether (60–90 $^\circ\text{C}$) as eluent to yield 4 (1.2255 g, 90%) as a white solid. Mp: 42–44 $^\circ\text{C}$. ^1H NMR (CDCl_3 , 400 MHz): δ 7.61 (d, J = 0.8 Hz, 1H), 7.41 (d, J = 0.8 Hz, 1H), 7.26 (d, J = 4 Hz, 1H), 7.17 (d, J = 4 Hz, 1H), 0.35 (s, 9H), 0.34 (s, 9H). ^{13}C NMR (100 MHz, CDCl_3): δ 144.15, 141.47, 138.83, 136.87, 134.64, 132.99, 124.98, 124.44, -0.07 , -0.12 . IR (KBr): 3095, 3057, 2955, 2895 (C–H) cm^{-1} . HRMS (EI^+): m/z calcd for $[\text{C}_{14}\text{H}_{22}\text{S}_2\text{Si}_2]$ 310.0702, found 310.0698.

Synthesis of COTh-1 and COTh-2 from 4. *n*-BuLi (2.39 M in hexane, 0.33 mL, 0.79 mmol, 2.2 equiv) was added to 4 (0.1130 g, 0.36 mmol, 1.0 equiv) in dry ethyl ether (30 mL) at -78°C . After 1 h at -78°C , the reaction mixture was heated to 60 $^\circ\text{C}$ for 2 h and then cooled to -78°C for 0.5 h. After that, dry CuCl_2 (0.1500 g, 1.12 mmol, 3.1 equiv) was added. The reaction mixture was kept at -78°C for 1 h and then warmed slowly to ambient temperature overnight. The reaction mixture was quenched with CH_3OH , extracted with ethyl ether (3 \times 25 mL), and finally dried over anhydrous MgSO_4 . After the solvent was removed in vacuo, the residue was purified by long column chromatography on silica gel with petroleum ether (60–90 $^\circ\text{C}$) as eluent to yield COTh-1 (0.0448 g, 40%) as a light yellow solid and COTh-2 (0.0204 g, 18%) as a pale white solid. COTh-1. Mp > 300 $^\circ\text{C}$. ^1H NMR (CDCl_3 , 400 MHz): δ 7.08 (s, 2H), 7.01 (s, 2H), 0.32 (s, 18H), 0.31 (s, 18H); ^{13}C NMR (100 MHz, CDCl_3): δ 142.68, 140.72, 140.19, 137.73, 137.64, 137.16, 136.85, 134.89, -0.12 , -0.23 . IR (KBr): 2956, 2925, 2853 (C–H) cm^{-1} . HRMS (MALDI/DHB): m/z calcd for $[\text{C}_{28}\text{H}_{40}\text{Si}_4\text{S}_4]$ 616.1090, found 616.1084. COTh-2: Mp > 300 $^\circ\text{C}$. ^1H NMR (CDCl_3 , 400 MHz): δ 7.05 (s, 4H), 0.32 (s, 36H). ^{13}C NMR (100 MHz, CDCl_3): δ 141.52, 140.77, 137.55, 134.06,

-0.17 . IR (KBr): 2954, 2895 (C–H) cm^{-1} . HRMS (MALDI/DHB): m/z calcd for $[\text{C}_{28}\text{H}_{40}\text{Si}_4\text{S}_4]$ 616.1090, found 616.1084.

Synthesis of 3-(4,4,5,5-Tetramethyl-1,3,2-dioxaborolan-2-yl)-5-trimethylsilylthiophene (5). *n*-BuLi (2.41 M in hexane, 1.03 mL, 2.49 mmol, 1.0 equiv) was added to 3 (0.5850 g, 2.49 mmol, 1.0 equiv) in dry ethyl ether (40 mL) at -78°C . After 2 h at -78°C , the homogeneous reaction mixture was treated with bis(pinacolato)diboron (0.6316 g, 2.49 mmol, 1.0 equiv, dissolved in 10 mL dry ethyl ether) and then warmed slowly to ambient temperature overnight. The reaction mixture was quenched with water, extracted with ethyl ether (3 \times 35 mL), and finally dried over anhydrous MgSO_4 . After the solvent was removed in vacuo, the residue was purified by column chromatography on silica gel with petroleum ether (60–90 $^\circ\text{C}$) as eluent to yield 5 (0.5616 g, 80%) as a white solid. Mp: 98–99 $^\circ\text{C}$. ^1H NMR (CDCl_3 , 400 MHz): δ 8.15 (d, J = 0.8 Hz, 1H), 7.56 (d, J = 0.8 Hz, 1H), 1.34 (s, 12H), 0.32 (s, 9H). ^{13}C NMR (100 MHz, CDCl_3): δ 141.66, 140.53, 139.27, 83.60, 24.81, -0.04 . IR (KBr): 2981, 2958 (C–H) cm^{-1} . HRMS (EI^+): m/z calcd for $[\text{C}_{13}\text{H}_{23}\text{O}_2\text{Si}^{10}\text{B}]$ 281.1317, found 281.1320.

Synthesis of 7. Compound 5 (0.4024 g, 1.43 mmol, 2.51 equiv), compound 6 (0.2670 g, 0.57 mmol, 1.0 equiv), K_2CO_3 (0.3940 g, 2.85 mmol, 5.0 equiv), and $\text{Pd}(\text{PPh}_3)_4$ (0.0527 g, 45.60 μmol , 0.08 equiv) were added into THF (16 mL) and water (2 mL) under argon. The mixture was stirred for 30 h at 110 $^\circ\text{C}$. After being quenched with water, the reaction mixture was extracted with chloroform (3 \times 30 mL) and finally dried over anhydrous MgSO_4 . After the solvent was removed in vacuo, the residue was purified by column chromatography on silica gel with petroleum ether (60–90 $^\circ\text{C}$) as eluent to yield 7 (0.2750 g, 78%) as a white solid. Mp: 89–90 $^\circ\text{C}$. ^1H NMR (CDCl_3 , 400 MHz): δ 7.15 (d, J = 0.8 Hz, 2H), 7.05 (s, 2H), 6.91 (d, J = 0.8 Hz, 2H), 0.32 (s, 18H), 0.22 (s, 18H). ^{13}C NMR (100 MHz, CDCl_3): δ 140.26, 139.81, 137.67, 137.27, 135.95, 134.16, 133.99, 126.52, -0.09 , -0.19 . IR (KBr): 3115, 2955, 2895 (C–H) cm^{-1} . HRMS (TOF MS EI^+): m/z calcd for $[\text{C}_{28}\text{H}_{42}\text{Si}_4\text{S}_4]$ 618.1247, found 618.1254.

Synthesis of COTh-1 from 7. *n*-BuLi (2.29 M in hexane, 0.19 mL, 0.44 mmol, 2.2 equiv) was added to 7 (0.1213 g, 0.20 mmol, 1.0 equiv) in dry ethyl ether (30 mL) at -50°C , and then the mixture was warmed slowly to ambient temperature. After 2 h, the reaction mixture was cooled to -78°C for 0.5 h. After that, dry CuCl_2 (0.0791 g, 0.60 mmol, 3.0 equiv) was added. The reaction mixture was kept at -78°C for 1 h and then warmed slowly to ambient temperature overnight. The reaction mixture was quenched with CH_3OH , extracted with ethyl ether (3 \times 25 mL), and finally dried over anhydrous MgSO_4 . After the solvent was removed in vacuo, the residue was purified by column chromatography on silica gel with petroleum ether (60–90 $^\circ\text{C}$) as eluent to yield COTh-1 (0.0474 g, 39%) as a light yellow solid.

Synthesis of 8. *n*-BuLi (2.39 M in hexane, 0.63 mL, 1.50 mmol, 2.2 equiv) was added to 4 (0.2120 g, 0.68 mmol, 1.0 equiv) in dry ethyl ether (15 mL) at -78°C . After 1 h at -78°C , the reaction mixture was heated to 60 $^\circ\text{C}$ for 2 h and then cooled to -78°C . After that, dry I_2 (0.5190 g, 2.04 mmol, 3.0 equiv) was added, and then the reaction mixture was warmed slowly to ambient temperature overnight. The reaction mixture was quenched with CH_3OH and extracted with ethyl ether (3 \times 25 mL), and the organic phase was washed with saturated $\text{Na}_2\text{S}_2\text{O}_3$ solution and H_2O and dried over anhydrous MgSO_4 . After the solvent was removed in vacuo, the residue was purified by column chromatography on silica gel with petroleum ether (60–90 $^\circ\text{C}$) as eluent to yield 8 (0.3620 g, 94%) as a light yellow solid. Mp: 76–78 $^\circ\text{C}$. ^1H NMR (CDCl_3 , 400 MHz): δ 7.23 (s, 1H), 7.06 (s, 1H), 0.34 (s, 9H), 0.32 (s, 9H). ^{13}C NMR (100 MHz, CDCl_3): δ 146.88, 143.22, 142.27, 141.67, 141.52, 136.18, 83.24, 83.19, -0.21 , -0.23 . HRMS (EI^+): m/z calcd for $[\text{C}_{14}\text{H}_{20}\text{Si}_2\text{S}_2\text{I}_2]$ 561.8635, found 561.8636.

Synthesis of 9. Compound 8 (0.2000 g, 0.36 mmol 1.0 equiv), compound 5 (0.3010 g, 1.07 mmol, 3.0 equiv), K_2CO_3 (0.2100 g, 1.52 mmol, 4.2 equiv), and $\text{Pd}(\text{PPh}_3)_4$ (0.0328 g, 28.38 μmol , 0.08 equiv) were added in THF (10 mL) and water (2 mL) under argon. The mixture was stirred at 100 $^\circ\text{C}$ for 15 h. After being quenched with water, the reaction mixture was extracted with chloroform (3 \times 25

mL) and finally dried over anhydrous MgSO_4 . After the solvent was removed in vacuo, the residue was purified by column chromatography on silica gel with petroleum ether (60–90 °C) as eluent to yield **9** (0.1870 g, 85%) as a white solid. Mp: 66–68 °C. ^1H NMR (CDCl_3 , 400 MHz): δ 7.32 (s, 1H), 7.13 (d, $J = 0.8$ Hz, 1H), 7.12 (d, $J = 0.8$ Hz, 1H), 7.11 (s, 1H), 6.88 (d, $J = 0.8$ Hz, 1H), 6.86 (d, $J = 0.8$ Hz, 1H), 0.34 (s, 9H), 0.32 (s, 9H), 0.21 (s, 9H), 0.20 (s, 9H). ^{13}C NMR (100 MHz, CDCl_3): δ 141.70, 139.93, 139.67, 139.27, 137.98, 137.81, 137.74, 137.57, 136.19, 135.56, 135.05, 134.24, 134.10, 131.31, 127.00, 126.44, -0.05, -0.12, -0.14, -0.19. IR (KBr): 2956, 2926, 2898, 2855 (C–H) cm^{-1} . HRMS (MALDI/DHB): m/z calcd for $[\text{C}_{28}\text{H}_{42}\text{Si}_4\text{S}_4]$ 618.1247, found 618.1241.

Synthesis of COTH-3. *n*-BuLi (2.50 M in hexane, 0.21 mL, 0.53 mmol, 2.2 equiv) was added to **9** (0.1500 g, 0.24 mmol, 1.0 equiv) in dry ethyl ether (25 mL) at -50 °C. After that, the reaction mixture was warmed slowly to ambient temperature, kept for 2 h, and then cooled to -78 °C for 0.5 h. Then dry CuCl_2 (0.1000 g, 0.74 mmol, 3.1 equiv) was added. The reaction mixture was kept at -78 °C for 1 h and then warmed slowly to ambient temperature overnight. The reaction mixture was quenched with CH_3OH , extracted with ethyl ether (3 \times 20 mL), and finally dried over anhydrous MgSO_4 . After the solvent was removed in vacuo, the residue was purified by column chromatography on silica gel with petroleum ether (60–90 °C) as eluent to yield **COTH-3** (0.0568 g, 38%) as a yellow solid. Mp > 300 °C. ^1H NMR (CDCl_3 , 400 MHz): δ 7.09 (s, 1H), 7.05 (s, 1H), 7.05 (s, 1H), 7.02 (s, 1H), 0.33 (s, 18H), 0.32 (s, 18H). ^{13}C NMR (100 MHz, CDCl_3): δ 142.51, 140.95, 140.85, 140.83, 140.60, 138.28, 137.68, 137.67, 137.54, 137.06, 136.89, 136.77, 136.68, 134.57, 134.42, -0.11, -0.17, -0.23. IR (KBr): 2956, 2896 (C–H) cm^{-1} . HRMS (MALDI/DHB): m/z calcd for $[\text{C}_{28}\text{H}_{40}\text{Si}_4\text{S}_4]$ 616.1090, found 616.1084.

Synthesis of 11. *n*-BuLi (2.50 M in hexane, 0.15 mL, 0.38 mmol, 1.0 equiv) was added to 2',3-dibromo-5,5'-bistrimethylsilyl-2,3'-bithiophene (**10**) (0.1751 g, 0.38 mmol, 1.0 equiv) in THF (25 mL) at -78 °C. After 2 h at -78 °C, the reaction mixture was treated with isopropoxyboronic acid pinacol ester (0.0912 g, 0.49 mmol, 1.3 equiv) and then warmed slowly to ambient temperature overnight. The reaction mixture was quenched with water, extracted with dichloromethane (3 \times 25 mL), and finally dried over anhydrous MgSO_4 . After the solvent was removed in vacuo, the residue was purified by column chromatography on silica gel via gradient elution using the solvent mixture (4:1 petroleum ether/dichloromethane) as eluent to yield **11** (0.1002 g, 52%) as a liquid. ^1H NMR (CDCl_3 , 400 MHz): δ 7.39 (s, 1H), 7.10 (s, 1H), 1.27 (s, 12H), 0.33 (s, 18H). ^{13}C NMR (100 MHz, CDCl_3): δ 146.94, 141.94, 139.91, 139.10, 110.30, 83.93, 24.73, -0.18, -0.31. IR: 3063, 2977, 2957, 2928, 2852 (C–H) cm^{-1} . HRMS (EI^+): m/z calcd for $[\text{C}_{20}\text{H}_{32}\text{O}_2\text{S}_2\text{Si}_2\text{Br}_2\text{B}]$ 514.0659, found 514.0641.

Computational Details. The geometry optimization of model compounds **COTH-1** to **COTH-4** were performed using B3LYP/6-31G(d)^{25,26} level of theory. The transition-state structures were optimized using a TS keyword. All optimized geometries are characterized as stationary points or transition state on the potential energy surface (PES) confirmed by with vibrational frequency calculations with no imaginary or only an imaginary frequency, respectively. Time dependent density functional theory (TD-DFT) calculations were performed on the equilibrium ground state geometries of **COTH-1** at 6-31+g(d,p) levels with the local generalized-gradient approximations (GGA) mPWPW91,^{27,28} the nonlocal hybrid GGA B3LYP,^{25,26} and the hybrid Coulomb-attenuating CAM-B3LYP²⁹ functional. Absorption spectra were simulated considering the 30 vertical excitations from the ground state by using the polarizable continuum model (PCM)^{30–32} in chloroform solution. According to experimental UV–vis results, the combined TD-B3LYP/PCM calculations exhibit evidently better performance compared to the ones based on mPWPW91 and CAM-B3LYP. Thus, the natural transition orbitals (NTO)³³ and charge difference density (CDD)³⁴ analyses of the excited states based on TD-B3LYP/PCM were used to assign the transition nature. Nucleus-independent chemical shifts (NICS)³⁵ values of molecules and

transition states were obtained at the B3LYP/6-311+G(d,p) level through the gauge-including atomic orbital method (GIAO).^{36,37} Initially, probes ($\text{Bq}'\text{s}$) were placed at the nonweighted means of the carbon atoms on the cyclooctatetraene (NICS(0)), and later, 1 Å above the NICS(0), denoted as NICS(1) (see Figures S36–S39, Supporting Information). All calculations were carried out with Gaussian 03³⁸ except for TDDFT/CAM-B3LYP calculations, which employed the Gaussian 09 suite of programs.³⁹

■ ASSOCIATED CONTENT

Supporting Information

Characterization of all compounds and crystallographic CIF files of **COTH-1** to **COTH-3**. Cartesian coordinates, frontier molecular orbitals, electronic transitions, and NICS in the ground state and in the transition state. This material is available free of charge via the Internet at <http://pubs.acs.org>.

■ AUTHOR INFORMATION

Corresponding Authors

*E-mail: songjs@henu.edu.cn. Phone: (0086)-371-23897112 (o). Fax: 23881358.

*E-mail: kyh@hytc.edu.cn. Phone: (0086)-517-83525663 (o). Fax: 83525663.

*E-mail: hwang@henu.edu.cn. Phone: (0086)-371-23897112 (o). Fax: 23881358.

Author Contributions

[†]Y. Wang and J. Song contributed equally to this work.

Notes

The authors declare no competing financial interest.

■ ACKNOWLEDGMENTS

This research was supported by the NSFC (21270255, U1204212), the Program for SRFDP (20124103110004), and the CPSF (2011M500787). We also thank Prof. Z. M. Su, Institute of Functional Material Chemistry, NENU, for use of the CAM-B3LYP functional in the Gaussian 09 program suite.

■ REFERENCES

- (1) (a) Harpham, M. R.; Süzer, Ö.; Ma, C.-Q.; Bäuerle, P.; Goodson, T., III. *J. Am. Chem. Soc.* **2009**, *131*, 973. (b) Ma, C.-Q.; Mena-Osteritz, E.; Debaerdemaeker, T.; Wienk, M. M.; Janssen, R. A. J.; Bäuerle, P. *Angew. Chem., Int. Ed.* **2007**, *46*, 1679. (c) Matsumoto, K.; Tanaka, T.; Kugo, S.; Inagaki, T.; Hirao, Y.; Kurata, H.; Kawase, T.; Kubo, T. *Chem.—Asian J.* **2008**, *3*, 2024.
- (2) Wang, Z. H.; Shi, J. W.; Wang, J. G.; Li, C. L.; Tian, X. Y.; Cheng, Y. X.; Wang, H. *Org. Lett.* **2010**, *12*, 456.
- (3) (a) Rajca, A.; Wang, H.; Pink, M.; Rajca, S. *Angew. Chem., Int. Ed.* **2000**, *39*, 4481. (b) Miyasaka, M.; Pink, M.; Rajca, S.; Rajca, A. *Angew. Chem., Int. Ed.* **2009**, *48*, 5954. (c) Miyasaka, M.; Rajca, A.; Pink, M.; Rajca, S. *J. Am. Chem. Soc.* **2005**, *127*, 13806. (d) Rajca, A.; Miyasaka, M.; Pink, M.; Wang, H.; Rajca, S. *J. Am. Chem. Soc.* **2004**, *126*, 15211. (e) Miyasaka, M.; Pink, M.; Rajca, S.; Rajca, A. *Org. Lett.* **2010**, *12*, 3230.
- (4) Heinz, W.; Räder, H.-J.; Müllen, K. *Tetrahedron Lett.* **1989**, *30*, 159.
- (5) (a) Marsella, M. J.; Reid, R. J. *Macromolecules* **1999**, *32*, 5982. (b) Marsella, M. J.; Reid, R. J.; Estassi, S.; Wang, L. S. *J. Am. Chem. Soc.* **2002**, *124*, 12507.
- (6) Sygula, A.; Fronczek, F. R.; Sygula, R.; Rabideau, P. W.; Olmstead, M. M. *J. Am. Chem. Soc.* **2007**, *129*, 3842.
- (7) Nishiuchi, T.; Kuwatani, Y.; Nishinaga, T.; Iyoda, M. *Chem.—Eur. J.* **2009**, *15*, 6838.
- (8) Rapson, W. S.; Shuttleworth, R. G.; van Niekerk, J. N. *J. Chem. Soc.* **1943**, 326.

- (9) (a) Kauffmann, T.; Greving, B.; Kriegesmann, R.; Mitschker, A.; Woltermann, A. *Chem. Ber.* **1978**, *111*, 1330. (b) Wang, Y. G.; Wang, Z. H.; Zhao, D. F.; Wang, Z.; Cheng, Y. X.; Wang, H. *Synlett* **2007**, 2390. (c) Nishiuchi, T.; Tanaka, K.; Kuwatani, Y.; Sung, J.; Nishinaga, T.; Kim, D.; Iyoda, M. *Chem.—Eur. J.* **2013**, *19*, 4110. (d) Nishinaga, T.; Ohmae, T.; Aita, K.; Takase, M.; Iyoda, M.; Araib, T.; Kunugi, Y. *Chem. Commun.* **2013**, 49, 5354. (e) Lin, F.; Peng, H. Y.; Chen, J. X.; Chik, D. T. W.; Cai, Z. W.; Wong, K. M. C.; Yam, V. W. W.; Wong, H. N. C. *J. Am. Chem. Soc.* **2010**, *132*, 16383. (f) Rashidi-Ranjbar, P.; Man, Y.-M.; Sandstrom, J.; Wong, H. N. C. *J. Org. Chem.* **1989**, *54*, 4888. (g) Lai, C. W.; Lam, C. K.; Lee, H. K.; Mak, T. C. W.; Wong, H. N. C. *Org. Lett.* **2003**, *5*, 823.
- (10) Mouri, K.; Saito, S.; Yamaguchi, S. *Angew. Chem., Int. Ed.* **2012**, *51*, 5971.
- (11) Marsella, M. J. *Acc. Chem. Res.* **2002**, *35*, 944.
- (12) Li, C. L.; Shi, J. W.; Xu, L.; Wang, Y. G.; Cheng, Y. X.; Wang, H. *J. Org. Chem.* **2009**, *74*, 408.
- (13) Wu, R.; Schumm, J. S.; Pearson, D. L.; Tour, J. M. *J. Org. Chem.* **1996**, *61*, 6906.
- (14) Getmanenko, Y. A.; Tongwa, P.; Timofeeva, T. V.; Marder, S. R. *Org. Lett.* **2010**, *12*, 2136.
- (15) Sun, H. L.; Shi, J. W.; Zhang, Z. L.; Zhang, S.; Liang, Z. L.; Wan, S. S.; Cheng, Y. X.; Wang, H. *J. Org. Chem.* **2003**, *78*, 6271.
- (16) Ohmae, T.; Nishinaga, T.; Wu, M.; Iyoda, M. *J. Am. Chem. Soc.* **2010**, *132*, 1066.
- (17) (a) Rajca, A.; Safronov, A.; Rajca, S.; Wongsriratanakul, J. *J. Am. Chem. Soc.* **2000**, *122*, 3351. (b) Rajca, A.; Wang, H.; Bolshov, P.; Rajca, S. *Tetrahedron* **2001**, *57*, 3725. (c) Wen, J.-F.; Hong, W.; Yuan, K.; Mak, T. C. W.; Wong, H. N. C. *J. Org. Chem.* **2003**, *68*, 8918.
- (18) Xiao, S. Z.; Pink, M.; Wang, H.; Rajca, S.; Rajca, A. *J. Sulfur Chem.* **2008**, *29*, 425.
- (19) Liu, Y.; Wang, Y.; Wu, W.; Liu, Y.; Xi, H.; Wang, L.; Qiu, W.; Lu, K.; Du, C.; Yu, G. *Adv. Funct. Mater.* **2009**, *19*, 772.
- (20) (a) Cui, L.; Li, L. F.; Ai, S. Y.; Yin, H. S.; Ju, P.; Liu, T. *J. Solid State Electrochem.* **2011**, *15*, 1253. (b) Laviron, E. *J. Electroanal. Chem. Interfacial Electrochem.* **1979**, *101*, 19.
- (21) Yin, H. S.; Zhou, Y. L.; Ai, S. Y. *J. Electroanal. Chem.* **2009**, *626*, 80.
- (22) Sanghavi, B. J.; Sitaula, S.; Griep, M. H.; Karna, S. P.; Ali, M. F.; Swami, N. S. *Anal. Chem.* **2013**, *85*, 8158.
- (23) (a) Wang, Y.; Gao, D. W.; Shi, J. W.; Kan, Y. H.; Song, J. S.; Li, C. L.; Wang, H. *Tetrahedron* **2014**, *70*, 631. (b) Marsella, M. J.; Kim, I. T.; Tham, F. *J. Am. Chem. Soc.* **2000**, *122*, 974.
- (24) Chotana, G. A.; Kallepalli, V. A.; Maleczka, R. E., Jr.; Smith, M. R., III. *Tetrahedron* **2008**, *64*, 6103.
- (25) Becke, A. D. *Phys. Rev. A* **1988**, *38*, 3098.
- (26) Lee, C. T.; Yang, W. T.; Parr, R. G. *Phys. Rev. B* **1988**, *37*, 785.
- (27) Perdew, J. P.; Burke, K.; Ernzerhof, M. *Phys. Rev. Lett.* **1996**, *77*, 3865.
- (28) Adamo, C.; Barone, V. *J. Chem. Phys.* **1998**, *108* (2), 664.
- (29) Yanai, T.; Tew, D. P.; Handy, N. C. *Chem. Phys. Lett.* **2004**, *393*, 51.
- (30) Cancès, E.; Mennucci, B.; Tomasi, J. *J. Chem. Phys.* **1997**, *107*, 3032.
- (31) Cossi, M.; Barone, V.; Mennucci, B.; Tomasi, J. *Chem. Phys. Lett.* **1998**, *286*, 253.
- (32) Mennucci, B.; Tomasi, J. *J. Chem. Phys.* **1997**, *106*, 5151.
- (33) Martin, R. L. *J. Chem. Phys.* **2003**, *118*, 4775.
- (34) Beenken, W. J. D.; Pullerits, T. *J. Phys. Chem. B* **2004**, *108*, 6164.
- (35) Schleyer, P. v. R.; Maerker, C.; Dransfeld, A.; Jiao, H.; Hommes, N. J. R. v. E. *J. Am. Chem. Soc.* **1996**, *118*, 6317.
- (36) Wolinski, K.; Hilton, J. F.; Pulay, P. *J. Am. Chem. Soc.* **1990**, *112*, 8251.
- (37) Cheeseman, J. R.; Trucks, G. W.; Keith, T. A.; Frish, J. M. *J. Chem. Phys.* **1996**, *104*, 5497.
- (38) Frisch, M. J.; Trucks, G. W.; Schlegel, H. B. et al. *Gaussian 03*, revision C.02; Gaussian, Inc.: Wallingford, CT, 2004 (see the Supporting Information for the full reference).
- (39) Frisch, M. J.; Trucks, G. W.; Schlegel, H. B. et al. *Gaussian 09*, revision A.02; Gaussian, Inc.: Wallingford, CT, 2008 (see the Supporting Information for the full reference).